Binding of dynein intermediate chain 2 to paxillin controls focal adhesion dynamics and migration

Carine Rosse[1,*,‡], Katrina Boeckeler[1], Mark Linch[1], Simone Radtke[1], David Frith[2], Karin Barnouin[2], Ali Sayed Morsi[3], Majid Hafezparast[3], Michael Howell[4] and Peter J. Parker[1,5,‡]

[1]Protein Phosphorylation Laboratory, Cancer Research UK, London Research Institute, London WC2A 3PX, UK
[2]Protein Analysis Laboratories, Cancer Research UK, London Research Institute, South Mimms EN6 3LD, UK
[3]Department of Biochemistry, School of Life Sciences, John Maynard Smith Building, University of Sussex, Brighton BN1 9RQ, UK
[4]High-Throughput Screening Laboratory, Cancer Research UK, London Research Institute, London WC2A 3LY, UK
[5]Division of Cancer Studies KCL, New Hunt's House, Guy's Campus, London WC2A 3LY, UK

*Present address: CNRS UMR144, Institut Curie, 75248 Paris Cedex 05, France
‡Authors for correspondence (peter.parker@cancer.org.uk; carine.rosse@curie.fr)

Accepted 7 April 2012
Journal of Cell Science 125, 3733–3738

doi: 10.1242/jcs.089557

Summary

In migrating NRK cells, aPKCs control the dynamics of turnover of paxillin-containing focal adhesions (FA) determining migration rate. Using a proteomic approach (two-dimensional fluorescence difference gel electrophoresis), dynein intermediate chain 2 (dynein IC2) was identified as a protein that is phosphorylated inducibly during cell migration in a PKC-regulated manner. By gene silencing and co-immunoprecipitation studies, we show that dynein IC2 regulates the speed of cell migration through its interaction with paxillin. This interaction is controlled by serine 84 phosphorylation, which lies on the aPKC pathway. The evidence presented thus links aPKC control of migration to the dynein control of FA turnover through paxillin.

Key words: aPKCs, Dynein, Microtubules, Migration, Paxillin

Introduction

In order for cells to achieve efficient migration, cell adhesion and detachment must be properly coordinated. Cells attach to the extracellular matrix via focal contacts, which can mature into focal adhesions (Pollard and Borisy, 2003; Schwartz and Horwitz, 2006; Vicente-Manzanares et al., 2007; Zaidel-Bar et al., 2004).

The atypical protein kinase C (PKC) isoforms (aPKCζ/ι) can be activated through Par6/cdc42 (Yamanaka et al., 2001). Interactions with the Par6/Par3 complex have implicated aPKC isoforms in a number of polarity (Suzuki and Ohno, 2006) and migratory (Nishimura and Kaibuchi, 2007; Rosse et al., 2009) models. Recently, we demonstrated that aPKC interacts via the scaffold protein Kibra with the Exocyst complex, a complex of eight proteins which facilitates regulated exocytosis to regions of membrane activity (Guo and Novick, 2004; Munson and Novick, 2006; Rosse et al., 2009; Sugihara et al., 2002; TerBush et al., 1996; Zuo et al., 2006). There is a mutual dependence of aPKC and Exocyst for their behaviour in migratory cells and this is associated with their mutually dependent regulation of the delivery of signals to the leading edge of migrating cells. Key regulatory processes under the control of these local aPKC/Exocyst-dependent signals have been identified. In particular focal adhesion (FA) stability represents a critical migratory output of the aPKC/Exocyst pathway (Rossé et al., 2006; Rosse et al., 2009). Interestingly, Par3 was shown to be associated with the dynein complex via light intermediate chain 2 (LIC2) and contributes to the local regulation of microtubule (MT) dynamics at NIH 3T3 cell–cell contacts and also the proper positioning of the centrosome at the cell centre (Schmoranzer et al., 2009). Cells contain distinct dynein complexes distinguished by different combinations of subunit isoforms and probably make possible specific regulation of dynein motor activity and/or cargo binding (Ha et al., 2008). Here we show that dynein intermediate chain 2 (dynein IC2) interacts in an aPKC-regulated fashion with paxillin, controlling FA disassembly.

Results and Discussion

Dynein IC2 is phosphorylated and required during NRK cell migration

Through a 2D-DIGE screen, dynein IC2 was identified as a phosphoprotein induced by migration in a manner sensitive to PKC inhibition (Fig. 1A–C). We determined the requirement for dynein IC2 in NRK cell migration by knock down of dynein IC2 using a smart pool (Fig. 2C); this resulted in a cell migration defect of ~30%, compared to the luciferase control, as assessed in a monolayer wound healing model (Fig. 2A,B; supplementary material Movie 1). The defect is about 60% as assessed in migration across porous membranes (Fig. 2D,E) using either a short-interfering RNA (siRNA) smart pool or an individual siRNA (Fig. 2C). This effect was observed without affecting the persistence of the cells (Fig. 2B). The effect of the depletion of dynein IC2 on cell migration is also the consequence of the impairment of the dynein complex, the knock down of dynein IC2 triggers the depletion of the dynein heavy chain (supplementary material Fig. S2C) without affecting the dynactin subunit p150 glued (supplementary material Fig. S2D). To address the specificity of siRNAs against dynein IC2 and to exclude any possible off-target effect of the siRNAs, we tested whether the effects of dynein IC2 siRNAs on cell migration could be rescued

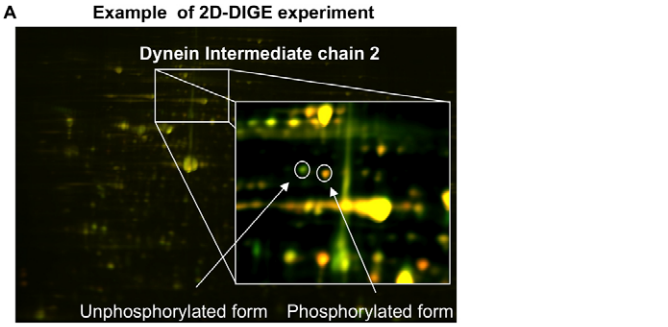

D

Migration conditions _ Dynein IC2 Immunoprecipitation		
58% coverage	**Modifications**	**Mascot Ion score**
(R)ADAEEEAATRIPA(-)		54,14
(M)sDKSELKAELER(K)	Acetyl	74.69
(R)TLAEINASR(A)		89.53
(R)DLEDKEGEIQAGAK(L)		107.55
(K)ITQVDFPPR(E)		75.54
(R)ALSEQINIFFDYSGR(D)		83.08
(K)IcSWSLDmLSHPQDSMELVHK(Q)	Carbamidomethyl , Oxidation	60.84
(K)SVSTPSEAGSQDSGDGAVGSR(T)		170.87
(R)TLAEINASRADAEEEAATR(I)		104.11
(R)TPLSAAAHTHPVYcVNVVGTQNAHNLISISTDGK(I)	Carbamidomethyl	89.51
(K)qQILHSEEFLSFFDHSTR(I)	Pyro-cmC	62.43
(R)LDLWNLNNDTEVPTASISVEGNPALNR(V)		52.36
(K)TTPEYVFHcQSAVmSATFAK(F)	Carbamidomethyl, Oxidation	87.44
(K)EAAVSVQEESDLEK(K)		115.27
(K)FHPNLVVGGTYSGQIVLWDNR(S)		62.65
(R)ALSEQINIFFDYSGRDLEDKEGEIQAGAK(L)		67.81
(K)EDEEEEDDVAAPKPPVEPEEEK(I)		108.22
(R)TPLSAAAHTHPVYcVNVVGTQNAHNLISISTDGK(I)	Carbamidomethyl	93.8
(R)EAEALLQSMGLTTDSPIVPPPMSPSSK(S)		88.9
(R)EAEALLQSmGLTTDSPIVPPPmSPSSK(S)	**Oxidation , Oxidation, Phospho**	**102.34**
(K)AVAVTSmSFPVGDVNNFVVGSEEGSVYTAcR(H)	Oxidation , Carbamidomethyl	182.84
(R)EIAVGDSEGQIVIYDVGEQIAVPR(N)		170.54

Fig. 1. Phosphorylation of dynein IC2 during cell migration. (**A**) Two-dimensional gel electrophoresis pattern of proteins from migrating NRK cells from a scratch wound assay. (**B**,**C**) Graphs representing the mean of four experiments for the phosphorylated spot (B) or the unphosphorylated spot (C) under the six conditions [6 h migration, 3 h migration or no migration, each with or without Gö6983 at 5 μM for the duration of the experiment (6 h)]. (**D**) Coverage of dynein IC2 peptides present in migrating cells.

with GFP–dynein IC1 which is resistant to the siRNAs targeting dynein IC2 (we note that the ectopic expression of dynein IC2 was not sufficient in terms of transfection efficiency, hence we resorted to testing the closest homolog of dynein IC2, i.e. dynein IC1). This isoform of dynein is mainly neuronal and is not detected in NRK cells (data not shown). Real-time imaging of wound-healing assays was used 72 hours post siRNA transfection (and 48 hours post DNA transfection), to examine directly the consequences of dynein IC2 depletion with GFP or GFP–dynein IC1 expressed. As shown in supplementary material Fig. S1B, in contrast to control cells, GFP–dynein IC1-positive cells displayed normal migration despite knock down of dynein IC2. The depletion of the endogenous dynein IC2 was similar whether GFP or GFP–dynein IC1 was ectopically expressed (supplementary material Fig. S1A). This validates the siRNA specificity and thus, we can conclude that dynein IC2 is indeed required for optimal cell migration, influencing the speed of migration. Interestingly we observed an additive effect on cell migration with the depletion of dynein IC2 and the inhibition of all PKCs except the aPKCs (using the inhibitor BIM1; Fig. 2F). Whereas when all the PKCs including aPKCs are inhibited, the depletion of dynein IC2 does not further increase the inhibition of cell migration (Fig. 2F). This result reinforces the idea that dynein IC2 is a downstream target of aPKCs on a promigratory pathway.

We found recurrently in mass spectrometry analyses of dynein IC2 the phosphopeptide EAEALLQSMGLTTDSPIVPPPMSPSSK, as also described previously (Vaughan et al., 2001); this phosphopeptide appeared to contain just one occupied phosphorylation site (Fig. 1D). Label-free quantification of the mass spectrometric ion abundance of this phosphopeptide indicates that it is increased about three times during cell migration compared to non-migrating cells or migrating cells treated with Gö6983 (data not shown). Hence dynein IC2 serine 84 (in bold and underlined: EAEALLQSMGLTTDSPIVPPPMSPS**S**K; serine 83 for the equivalent site in dynein IC1) was the serine phosphorylated in a Gö6983-sensitive manner. Antibodies against this phosphorylation site were generated. In the absence of aPKCs, we observed less phosphorylation of serine 84 of dynein IC2 during cell migration (supplementary material Fig. S2F). To investigate if this phosphorylation influenced migration, GFP alone, GFP–dynein IC1-WT, GFP–dynein IC1-S83A and GFP–dynein IC1-S83E were expressed in NRK cells. The efficiency of transfection is around 80% for the GFP alone and around 40% for the dynein IC constructs (supplementary material Fig. S1C). The overexpression of the GFP–dynein IC1-S83A significantly inhibited NRK cell migration ($P<0.001$; supplementary material Fig. S1D), whereas GFP–dynein IC1 and GFP–dynein IC1-S83E did not have a significant effect in comparison with GFP alone. This behaviour is indicative of a requirement for dynein IC1-S83 phosphorylation (and by inference dynein IC2 S84) during migration.

Dynein IC2 interacts with paxillin and controls FA turnover under the control of aPKC

It was described previously (Nishimura and Kaibuchi, 2007; Rosse et al., 2009) that aPKC controls the dynamics of paxillin at FA sites; siRNAs against aPKC or treatment with Gö6983 increased the number of paxillin patches. Here we tested if dynein IC2 shares this property of controlling FAs. Knock down of dynein IC2 in NRK cells increased the number of paxillin spots by ~40% (see Fig. 3A,B; supplementary material Fig. S2A) and their intensity (data not shown). These results are very similar to those obtained in a second cell model, RPE1 cells (retinal pigment epithelium cells) (supplementary material Fig. S3A,B, Fig. S2B). Here the depletion of sec5 serves as a positive control. It appears that on delivery to the leading edge dynein IC2 is involved in controlling FA turnover, phenocopying aPKC knock down and hence linking aPKC action in delivering dynein IC2 (dynein–dynactin complex) with its control of FA turnover. Because the inhibition of aPKCs triggers an increase in the FA content of another marker, zyxin (Boeckeler et al., 2010), we analysed the effects of dynein IC2 depletion on zyxin and paxillin at FAs (Fig. 3D). Consistent with the effects of aPKC inhibition, in the absence of dynein IC2, the number of zyxin–paxillin containing FAs increased (Fig. 3D). Because the aPKCs are important for the destabilisation of FAs (Boeckeler et al., 2010), (Rosse et al., 2009), we analysed the effect of the depletion of dynein IC2 on the disassembly rate of paxillin at FAs during cell migration using total internal reflection fluorescence (TIRF) microscopy and taking into consideration the localisation of the

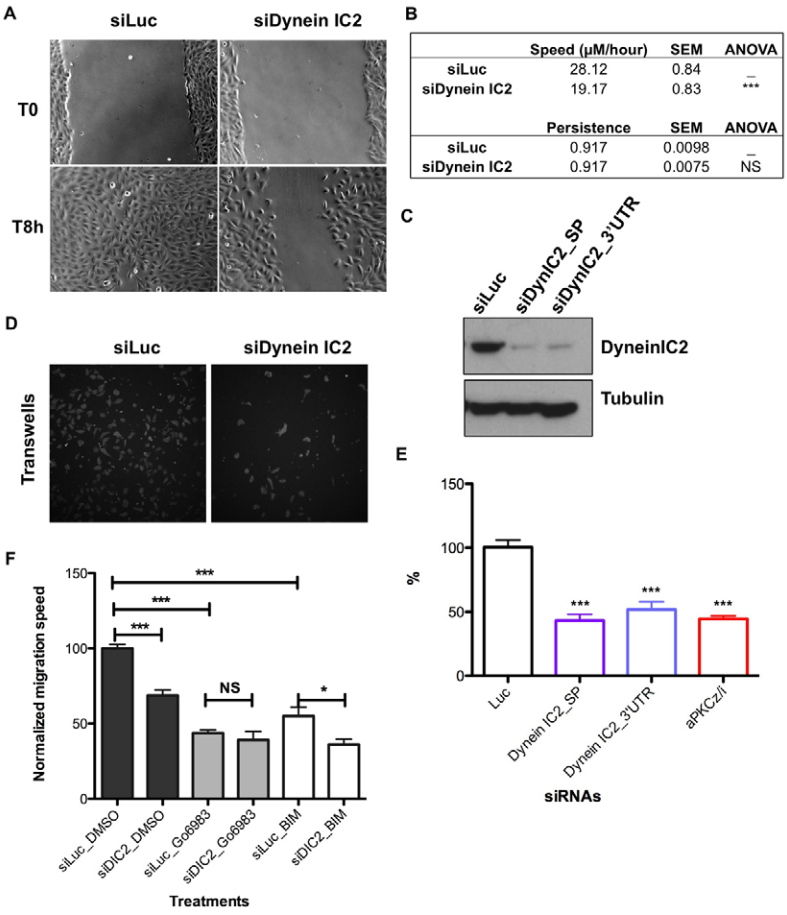

Fig. 2. Dynein IC2 is required for NRK cell migration. (**A**) Confluent monolayers of NRK cells transfected with the indicated siRNA were wounded 60 h post-transfection (T0), and wound healing was followed over time. T8 is 8 h post-wounding. The samples shown are representative of three independent experiments. (**B**) Quantification by single-cell tracking of migration speed and persistence during 8 h of migration (40 cells in two independent experiments) and the effects of dynein IC2 knock down. (**C**) siRNA dynein IC2 specificity and efficiency in NRK cells. Whole-cell extracts were analysed by immunoblotting with the indicated antibodies. (**D**,**E**) Quantitative NRK cell migration assays. At 48 h post-transfection with siRNAs, cells were place in Boyden chambers containing 0.5% serum. After 20 h, the cultures were fixed and cell migration was assessed by staining with phalloidin (D) as described in Materials and Methods. Error bars indicate the standard deviations from the means of three independent experiments. Statistically significant differences are indicated by an asterisk ($P<0.05$). (**F**) Real-time imaging of wound-healing assays was used 72 h post-siRNA-transfection to examine directly the consequences of dynein IC2 depletion with inhibition of PKCs using inhibitors [BIM inhibiting cPKCs and nPKCs, Gö6983 (5 μM) inhibiting cPKCs, nPKCs and aPKCs].

FAs (peripheral FA versus internal FA; Fig. 3C; supplementary material Movies 2, 3). First, we observed that the disassembly rate for the peripheral FAs is more than double the speed than for the internal FAs. When dynein IC2 is knocked down, the disassembly rate of the peripheral FAs is significantly decreased by about 40% whereas there is no significant effect on internal FAs. This result shows that dynein IC2 is involved specifically in the disassembly of the peripheral FAs during cell migration.

To investigate the basis of the effect of dynein IC2 on the dynamics of paxillin at the cell–substrate interface, assessment was made of the possible association of dynein IC2 and paxillin under control or migratory conditions (Fig. 4A,B). Paxillin was found to be more associated with dynein IC2 recovered from migrating cells. The interaction between dynein IC2 and paxillin was found to be significantly increased by about 40%, when cells were treated with Gö6983 (which inhibits c-, n- and aPKC; Fig. 4A,B) while BIMI (which inhibits c- and nPKC) had no effect (data not shown). This increase of interaction between paxillin and dynein IC2 is more prominent in non migrating cells; the interaction could not be further increased significantly in migrating cells. This result implies that the interaction between dynein IC2 and paxillin increased in the absence of aPKC activity. We confirmed this result using a siRNA approach. When aPKCs are knocked down, paxillin co-immunoprecipated more strongly with dynein IC2 (supplementary material Fig. S2E). To determine if dynein IC2 also interacts with components of the FA complexes classically associated with paxillin, focal adhesion kinase (FAK) was analysed and indeed found to associate with dynein IC2 (Fig. 4A). The interaction between FAK and dynein IC2 is increased during cell migration and more so in the absence of aPKC activity as is the interaction between dynein IC2 and p150 Glued (i.e. binding to the dynactin complex; Fig. 4A); this is consistent with previous studies (Vaughan et al., 2001).

Because FA disassembly could be mediated by dynamin2 (Ezratty et al., 2005; Ezratty et al., 2009), we determined whether the interaction between paxillin and dynein IC could be regulated by endocytosis. The interaction between dynein IC and paxillin increased on Dynasore (dynamin inhibitor) treatment compared to the DMSO control (Fig. 4C). This suggests that interaction is probably controlled by endocytosis/disassembly of the FA and this would be consistent with aPKC action at this juncture. This is consistent with the recent data (Osmani et al., 2010) showing that the localisation of aPKCs at the leading edge is dependent on membrane traffic.

To dissect whether (a)PKC control of site-specific phosphorylation of dynein IC2 was involved in this behaviour, we first established that ectopically expressed GFP–dynein IC2-WT interacted with endogenous paxillin. After a three hour scratch wound assay, GFP–dynein IC2-WT was immunoprecipitated with an antibody against GFP and paxillin was detected by western blot (note that the poor efficiency of transfection of dynein IC2 does not compromise the assessment of complex formation). To determine what influence phosphorylation of Serine 84 might have on this interaction, we tested non-phosphorylatable and

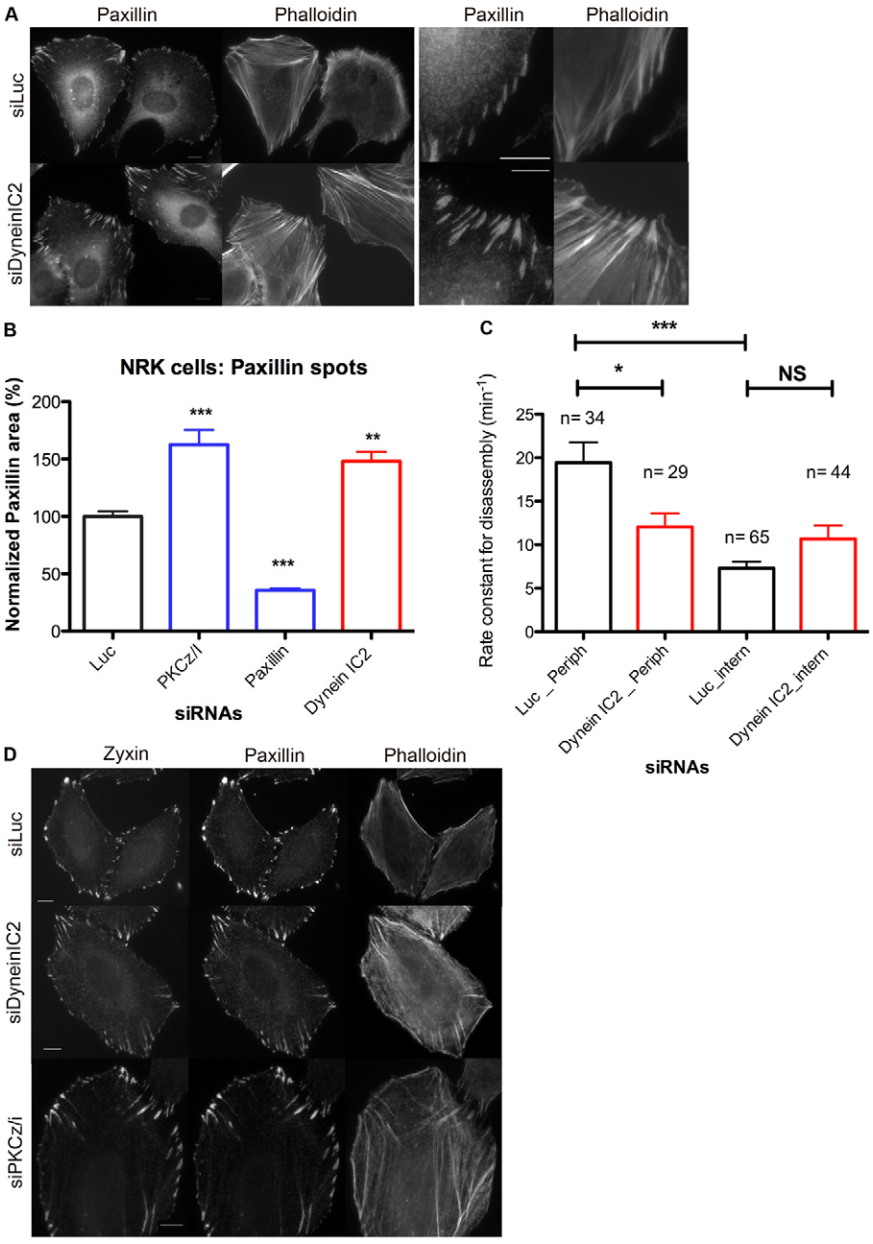

Fig. 3. Dynein IC controls the stability of the FAs. (**A**) Monolayers of NRK cells were transfected with the indicated siRNAs (20 nM) and immunostained for actin (phalloidin) and paxillin. All the pictures were taken with the same microscope settings. Scale bar: 5 μm. (**B**) Quantification of the number of spots of paxillin per cell and the area of stress fibres after depletion of aPKC and dynein IC2 in NRK cells. (**C**) Quantification of the disassembly rate of paxillin focal adhesions (stills from supplementary material Movies 2, 3) using TIRF microscopy. (**D**) Monolayers of NRK cells were transfected with the indicated siRNAs (20 NM) and immunostained for actin (phalloidin), zyxin and paxillin. All the images were taken with the same microscope settings. Scale bar: 5 μm.

phosphomimetic dynein IC2 mutants. GFP–dynein IC2-S84A was found to be more associated with paxillin than GFP–dynein IC2-WT (Fig. 4D) and the phosphomimetic GFP–dynein IC2-S84D did not associate with paxillin. To address where in the cell dynein IC2 interacts with paxillin, GFP–dynein IC2-WT or S84A and mCherry–paxillin were expressed in NRK cells, which were then fixed. We observed that GFP–dynein IC2-WT is partially associated with paxillin at FA sites (Fig. 4D; supplementary material Fig. S3C) and this is more pronounced for GFP–dynein IC2-S84A (Fig. 4D; supplementary material Fig. S3C), while GFP–dynein IC2-S84D is completely disengaged from the FA sites. The phospho-mimetic mutant of dynein IC2 cannot interact with paxillin, so is not a dominant negative for cell migration (supplementary material Fig. S1D).

There is an apparent disconnect between increased paxillin–dynein IC2 complex formation in migrating cells and increased phosphorylation of dynein IC2 via the aPKC pathway, which appears to suppress complex formation. However it is evident from our work with this migratory model that aPKC controls the delivery of cargo/signals to the leading edge and it is this aspect of its function that would promote complex formation. The subsequent phosphorylation of dynein IC2 would be consistent with both the dissociation of the complex (recycling components) and an increase in overall steady state phosphorylation due to the increased presence in this FA compartment. It is implicit that there is a pool of dynein IC2 which is neither in a paxillin complex, nor that is phosphorylated, but is available for recruitment to and engagement in this dynamic process. These results suggest that dynein IC2 interacts at least in part with paxillin at FA sites and that the phosphorylation on serine S84 destabilizes this interaction. To test further the idea that dynein IC2 could control the turnover of the FAs by controlling the endocytic rate, dynein IC2 was depleted in NRK cells and transferrin receptors and paxillin were immunostained (Fig. 4F). An accumulation of transferrin receptors

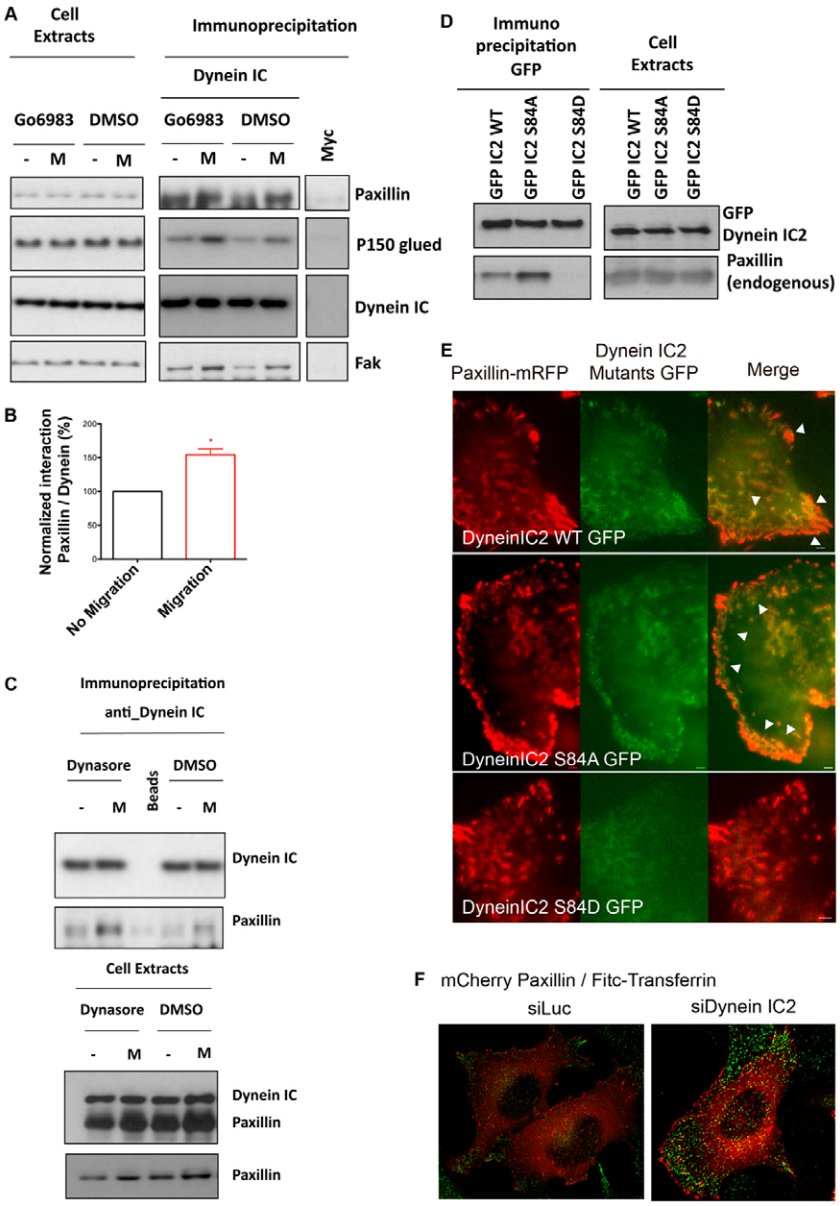

Fig. 4. Dynein IC interacts with and is colocalised with paxillin, under the control of endocytosis and aPKC. (**A**,**B**) As previously described (Rossé et al., 2006), a monolayer of confluent NRK cells was extensively scratched in the presence or absence of the aPKC inhibitor Gö6983 (5 µM), dynein IC was immunoprecipitated and paxillin, FAK and p150 Glued were detected by western blotting (A) and quantified using ImageJ software (B). M, migrating cells; –, non-migrating cells. (**C**) A monolayer of confluent NRK cells was extensively scratched in the presence or absence of the Dynasore (80 µM). Dynein IC2 was immunoprecipitated and paxillin was detected by western blotting (lower panel). The loading of the cell extracts (upper panel) was 10% of the input for immunoprecipitation. (**D**) A monolayer of confluent NRK cells overexpressing GFP–dynein IC2-WT, GFP–dynein IC2-S84A or GFP–dynein IC2-S84D was extensively scratched as in C and GFP–dynein IC2 was immunoprecipitated and endogenous paxillin was detected by western blotting. (**E**) GFP–dynein IC2-WT or -S84A or -S84D and mCherry–paxillin were expressed for 24 h in NRK cells. Cells were imaged by TIRF microscopy. GFP–dynein IC2-WT is partially associated with paxillin at FA sites, GFP–dynein IC2-S84A is more extensively associated with paxillin patches, whereas GFP–dynein IC2-S84D is not present in the FAs sites. Scale bar: 5 µm. (**F**) mCherry–paxillin was expressed for 24 h in NRK cells, which were then incubated with FITC–transferrin. Scale bar: 5 µm.

at FAs sites was observed when dynein IC2 was depleted indicative of a role for dynein IC2 in endocytosis at FAs.

The effect of dynein IC2 on paxillin dynamics is unexpected. The effect of Nudel at the FA is independent of dynein (Shan et al., 2009). Also, a block in dynein–cargo interaction induced no change in adhesion site dynamics in *Xenopus* fibroblasts, although inhibition of Kinesin 1 induced a dramatic increase in the size of substrate adhesions and is required for the delivery of a component(s) at the FAs that retards their growth or promotes their disassembly (Krylyshkina et al., 2002). This apparent discrepancy could be the result of a difference in balance between the delivery of components to the FA and the endocytosis of cargo, which will vary between cell types.

To conclude, dynein IC2 identified through a phosphoproteomics screen is a key component in the aPKC pathway involved in the turnover of focal adhesions during cell migration. Physically, dynein IC2 interacts with paxillin (directly or indirectly) and with some other components of the FAs such as FAK. This interaction occurs in an aPKC-regulated fashion and is associated with the turnover of focal adhesions. The interaction is also controlled by endocytosis and the depletion of dynein IC2 triggers the accumulation of transferrin receptor at the FAs. The data are consistent with a model in which the aPKC–Exocyst complex delivers the dynein–dynactin complex to FAs at the leading edge of migrating cells. The interaction there between paxillin and dynein IC2 facilitates the endocytosis of FAs with ensuing aPKC-dependent phosphorylation of dynein IC2, disruption of the paxillin interaction and hence recycling of these components (see supplementary material Fig. S4).

Materials and Methods

Cell culture and wound assay

Normal rat kidney (NRK) cells were cultivated in DMEM and 10% fetal calf serum. RPE1 cells were cultivated in DMEM–Ham's F12: 1-1 and 10% fetal calf serum. Wounds were inflicted by scratching the cell surface with a plastic pipette tip. Images were recorded using a Zeiss microscope and an Orca ER CCD camera (Hamamatsu). All inhibitor treatments were performed without pre-incubation. Quantification of the speed of individual cells was performed using Metamorph, Tracker and Mathematica software. Statistical analysis (ANOVA 2 factors) were

performed thanks to the Mathematica software. As an alternative readout, the migration speed was monitored by measuring the change in the area surrounding the wound over time, using Metamorph software. Statistical analysis (ANOVA 2 factors) were performed using Prism Software.

Immunofluorescence

Cells were fixed in 4% paraformaldehyde, permeabilised in 1% Triton X-100 and mounted using Prolong (Molecular Probes). Images were acquired using a confocal laser scanning microscope (LSM510, Carl Zeiss Inc.) equipped with a 63x/1.4 Plan-Apochromat oil immersion objective. Alexa 488 was excited with the 488-nm line of an argon laser, Cy3 was excited with a 543-nm HeNe laser and Cy5 was excited with a 633-nm HeNe laser. Each image represents a projection or a single section as indicated in the figure legend. For the (Fig. 4D,E), images were acquired using a Techniques Applications Eclipse 90i Upright Microscope (Nikon) equipped with Plan-Apochromat oil immersion objective Piezo Flexure Objective Scanner and a CCD Camera CoolSNAP HQ2. This microscope allows to do 3 D deconvolution. Each image represents a single section.

Boyden chamber assay

Boyden chamber assays were performed using transwell chambers with 8-μm-pore-size membranes (Biocoat Cell Culture Inserts; Becton Dickinson). The chambers were inserted into 24-well culture plates containing culture medium with 0.5% serum. The cells (10×10^4) were loaded into the upper compartments of the Boyden chambers. Non-migrated cells were removed with a cotton swab, and migrating cells were fixed and stained with phalloidin. Each condition was performed in triplicate. Cells were counted using a 10× objective; 9 fields per chamber were analysed.

Immunoprecipitation, immunodetection and antibodies

For whole-cell extracts, cells were lysed directly on plates in hot Laemmli sample buffer. For immunoprecipitation, cells were lysed in 20 mM Tris-HCl (pH 7.4), 100 mM NaCl, 1 mM $MgCl_2$, 0.1 mM dithiothreitol, 1% Triton X-100, and 10% glycerol). Quantification of the immunoprecipitates were performed using ImageJ. Antibodies were obtained from Santa Cruz (PKCζ/ι, paxillin, dynein IC), BD Biosciences (PKCι and rSec8) or Synaptic System (Zyxin). The different inhibitors were obtained from Calbiochem. Preparations of cell extracts and co-immunoprecipitations were performed according to published procedures (Rossé et al., 2006).

siRNAs and plasmid constructs

siRNAs were transfected at 20 nM with Hyperfect (Qiagen). siRNA sequences were: 5′-GCAAGCUGCUUGUCCAUAAdTdT-3′ (rPKCζ-1), 5′-GCAAACUGCUGGU-UCAUAAdTdT-3′ (rPKCι-1), 5′-GCCGUAGCCUUAUCGAGUtt-3′ (rdynein IC2 3′UTR). rDynein IC2-SP and Hs-dynein IC2 are smart pools from Dharmacon Thermofisher.

The mutagenesis on EGFP-tagged mouse dynein IC2c and mouse dynein IC1c was done with an Invitrogen kit using the oligos: IC2c-S84D sense: 5′-ctcctatg-tctccatccgacaagtcggtgagcacgc-3′; IC2c-S84A sense: 5′-cctatgtctccatccgccaagtc-ggtgagca-3′; IC1c-S83E sense: 5′-accctatgtctccctctgagaaatcagtgagcactcc-3′; IC1c-S83D sense: 5′-caacccctatgtctccctctgacaaatcagtgagcactcccag-3′; IC1c-S83A sense: 5′-cccaacccctatgtctccctctgcgaaatcagtgag-3′.

Analysis of paxillin spots and actin stress fibres

Where paxillin spots and actin stress fibres were quantified, an Array Scan II and the Cellomics analysis program were employed (Rosse et al., 2009). Statistical analyses (ANOVA 2 factors) were performed with Prism Software.

TIRF microscopy and analysis of the FAs disassembly rate

Stable NRK cell lines were grown in fibronectin-coated MatTek dishes to confluence. Cells were wounded to induce cell migration. Time-lapse TIRF imaging was performed on a custom setup as described previously (Montagnac et al., 2011) with a penetration depth of 150–300 nm. One pixel corresponds to 107.5 nm. To quantify the rates of focal adhesion assembly and disassembly, the fluorescence intensity of individual adhesions was measured over time using Metamorph. Changes in fluorescence intensity were normalized to the maximal value and plotted in semilogarithmic plots as a function of time. The rates were determined from the slopes of these graphs [disassembly: ln (max/minutes)] (Boeckeler et al., 2010).

Two-dimensional fluorescence difference gel electrophoresis and mass spectrometry

Performed as described by Akgül et al. (Akgül et al., 2009).

Acknowledgements

We thank the Light Microscopy Laboratory for their help and the Nikon Imaging Centre at the Institut Curie-CNRS. We are very grateful to all the members of the Protein Phosphorylation Laboratory, Giampietro Schiavo and Philippe Chavrier for stimulating discussions.

Funding

This work was supported by Cancer Research UK and a FEBS Longterm Fellowship to C.R.

Supplementary material available online at
http://jcs.biologists.org/lookup/suppl/doi:10.1242/jcs.089557/-/DC1

References

Akgül, B., Zigrino, P., Frith, D., Hanrahan, S. and Storey, A. (2009). Proteomic analysis reveals the actin cytoskeleton as cellular target for the human papillomavirus type 8. *Virology* **386**, 1-5.

Boeckeler, K., Rosse, C., Howell, M. and Parker, P. J. (2010). Manipulating signal delivery - plasma-membrane ERK activation in aPKC-dependent migration. *J. Cell Sci.* **123**, 2725-2732.

Ezratty, E. J., Partridge, M. A. and Gundersen, G. G. (2005). Microtubule-induced focal adhesion disassembly is mediated by dynamin and focal adhesion kinase. *Nat. Cell Biol.* **7**, 581-590.

Ezratty, E. J., Bertaux, C., Marcantonio, E. E. and Gundersen, G. G. (2009). Clathrin mediates integrin endocytosis for focal adhesion disassembly in migrating cells. *J. Cell Biol.* **187**, 733-747.

Guo, W. and Novick, P. (2004). The exocyst meets the translocon: a regulatory circuit for secretion and protein synthesis? *Trends Cell Biol.* **14**, 61-63.

Ha, J., Lo, K. W., Myers, K. R., Carr, T. M., Humsi, M. K., Rasoul, B. A., Segal, R. A. and Pfister, K. K. (2008). A neuron-specific cytoplasmic dynein isoform preferentially transports TrkB signaling endosomes. *J. Cell Biol.* **181**, 1027-1039.

Krylyshkina, O., Kaverina, I., Kranewitter, W., Steffen, W., Alonso, M. C., Cross, R. A. and Small, J. V. (2002). Modulation of substrate adhesion dynamics via microtubule targeting requires kinesin-1. *J. Cell Biol.* **156**, 349-360.

Montagnac, G., de Forges, H., Smythe, E., Gueudry, C., Romao, M., Salamero, J. and Chavrier, P. (2011). Decoupling of activation and effector binding underlies ARF6 priming of fast endocytic recycling. *Curr. Biol.* **21**, 574-579.

Munson, M. and Novick, P. (2006). The exocyst defrocked, a framework of rods revealed. *Nat. Struct. Mol. Biol.* **13**, 577-581.

Nishimura, T. and Kaibuchi, K. (2007). Numb controls integrin endocytosis for directional cell migration with aPKC and PAR-3. *Dev. Cell* **13**, 15-28.

Osmani, N., Peglion, F., Chavrier, P. and Etienne-Manneville, S. (2010). Cdc42 localization and cell polarity depend on membrane traffic. *J. Cell Biol.* **191**, 1261-1269.

Pollard, T. D. and Borisy, G. G. (2003). Cellular motility driven by assembly and disassembly of actin filaments. *Cell* **112**, 453-465.

Rossé, C., Hatzoglou, A., Parrini, M. C., White, M. A., Chavrier, P. and Camonis, J. (2006). RalB mobilizes the exocyst to drive cell migration. *Mol. Cell. Biol.* **26**, 727-734.

Rosse, C., Formstecher, E., Boeckeler, K., Zhao, Y., Kremerskothen, J., White, M. D., Camonis, J. H. and Parker, P. J. (2009). An aPKC-exocyst complex controls paxillin phosphorylation and migration through localised JNK1 activation. *PLoS Biol.* **7**, e1000235.

Schmoranzer, J., Fawcett, J. P., Segura, M., Tan, S., Vallee, R. B., Pawson, T. and Gundersen, G. G. (2009). Par3 and dynein associate to regulate local microtubule dynamics and centrosome orientation during migration. *Curr. Biol.* **19**, 1065-1074.

Schwartz, M. A. and Horwitz, A. R. (2006). Integrating adhesion, protrusion, and contraction during cell migration. *Cell* **125**, 1223-1225.

Shan, Y., Yu, L., Li, Y., Pan, Y., Zhang, Q., Wang, F., Chen, J. and Zhu, X. (2009). Nudel and FAK as antagonizing strength modulators of nascent adhesions through paxillin. *PLoS Biol.* **7**, e1000116.

Sugihara, K., Asano, S., Tanaka, K., Iwamatsu, A., Okawa, K. and Ohta, Y. (2002). The exocyst complex binds the small GTPase RalA to mediate filopodia formation. *Nat. Cell Biol.* **4**, 73-78.

Suzuki, A. and Ohno, S. (2006). The PAR-aPKC system: lessons in polarity. *J. Cell Sci.* **119**, 979-987.

TerBush, D. R., Maurice, T., Roth, D. and Novick, P. (1996). The Exocyst is a multiprotein complex required for exocytosis in Saccharomyces cerevisiae. *EMBO J.* **15**, 6483-6494.

Vaughan, P. S., Leszyk, J. D. and Vaughan, K. T. (2001). Cytoplasmic dynein intermediate chain phosphorylation regulates binding to dynactin. *J. Biol. Chem.* **276**, 26171-26179.

Vicente-Manzanares, M., Zareno, J., Whitmore, L., Choi, C. K. and Horwitz, A. F. (2007). Regulation of protrusion, adhesion dynamics, and polarity by myosins IIA and IIB in migrating cells. *J. Cell Biol.* **176**, 573-580.

Yamanaka, T., Horikoshi, Y., Suzuki, A., Sugiyama, Y., Kitamura, K., Maniwa, R., Nagai, Y., Yamashita, A., Hirose, T., Ishikawa, H. et al. (2001). PAR-6 regulates aPKC activity in a novel way and mediates cell-cell contact-induced formation of the epithelial junctional complex. *Genes Cells* **6**, 721-731.

Zaidel-Bar, R., Cohen, M., Addadi, L. and Geiger, B. (2004). Hierarchical assembly of cell-matrix adhesion complexes. *Biochem. Soc. Trans.* **32**, 416-420.

Zuo, X., Zhang, J., Zhang, Y., Hsu, S. C., Zhou, D. and Guo, W. (2006). Exo70 interacts with the Arp2/3 complex and regulates cell migration. *Nat. Cell Biol.* **8**, 1383-1388.